Scilight

Smart Materials and Devices

https://www.sciltp.com/journals/smd

Review

Superplasticity and Superelasticity of Structural-Functional Alloys

Chenlu Pan [1], Huixiang Lu [1], Ke Zhang [1], Aiying Chen [1], Zhiyi Ding [1,*], Feiyang Liu [2] and Andriy Lifanov [2]

[1] School of Materials and Chemistry, University of Shanghai for Science and Technology, Shanghai 200093, China
[2] Materials Academy, JITRI, Suzhou 215133, China
* Correspondence: zyding@usst.edu.cn

How To Cite: Pan, C.; Lu, H.; Zhang, K.; et al. Superplasticity and Superelasticity of Structural-Functional Alloys. *Smart Materials and Devices* **2025**, *1*(1), 3.

Received: 19 August 2025
Revised: 1 September 2025
Accepted: 24 September 2025
Published: 11 October 2025

Abstract: Shape-memory alloys (SMAs) inherently possess dual actuation and sensing capabilities. Excellent superelasticity and fatigue resistance are crucial for the service reliability and stability of SMAs. This review summarizes the microstructure, functional properties, strengthening mechanisms, and failure mechanisms of the most widely used NiTi-based SMA, Gum Metals, novel NiMn-based SMAs, and newly developed Fe-based alloys. The high strength and toughness of NiTi SMA contribute to its excellent fatigue performance, achieved through microalloying, structural design, and grain size engineering. Texture toughening strategies overcome the intergranular brittleness inherent in traditional NiMn-based SMAs. Alloy design strategies enable the development of iron-based superelastic alloys exhibiting near-constant critical stress temperature dependence, overcoming the conventional limitation in superelastic alloys where critical stress decreases significantly with decreasing temperature. The principles and implementation strategies for controlling superelasticity and superplasticity in SMAs provide valuable guidance for designing and applying structure-function-integrated materials.

Keywords: superelastic/superplastic alloy; fatigue resistance; NiTi; novel NiMn-based alloy; Fe-based alloy

1. Introduction

The exceptional mechanical properties of metallic materials are fundamental to achieving their functional characteristics. Traditional metallic materials exhibit limitations including poor stability, structural homogeneity, and limited adaptability, complicating their functional and engineering applications. Consequently, metallic materials exhibiting high strength, superplasticity, and superelasticity are developed through various strategies to achieve functional characteristics like the shape memory effect (SME) [1–3]. For structural materials, balancing strengthening with maintaining excellent superplasticity remains a persistent challenge. For SMAs, enhancing superelasticity and fatigue resistance while preserving functional characteristics continues to require strategic research efforts [4,5].

Recent research demonstrates that microalloying, heterostructure design, and oligocrystalline architectures effectively overcome the strength-ductility trade-off [6–14]. SMAs are intelligent metallic materials that integrate actuation and temperature sensing capabilities. Large reversible strains, including superelasticity, are achieved during loading-unloading cycles through reversible martensitic transformations. SMAs exhibit nonlinear stress-strain relationships during thermoelastic martensitic transformations. These characteristics enable SMA applications in (Figure 1) biomedicine [15], aerospace [16], and civil engineering [17] (Figure 1).

Fatigue resistance—the ability to withstand multiple loading-unloading cycles during transformation without performance degradation—is critical for SMA engineering applications. Functional degradation primarily results from dislocation accumulation and microcrack initiation during irreversible stress-induced processes at phase

interfaces, ultimately leading to material failure [18,19]. Moreover, achieving simultaneous high yield strength, functional stability, and fatigue resistance in SMAs remains challenging within uniform coarse-grained structures. Grain refinement [20–22], heterostructure design [7], and nanoprecipitation [23–28] can hinder dislocation motion, improve damage tolerance, enhance functional stability, and increase fatigue resistance.

This article provides a comprehensive review of the current research status of superelastic and superplastic shape memory alloys, with a focus on four systems: NiTi-based alloys, NiMn-based alloys, Ti-Nb-based Gum Metal, and Fe-based alloys. For each system, we analyze its key characteristics, application prospects, and current challenges, culminating in an outlook on future research directions. By systematically synthesizing existing research, this review aims to provide a foundation for designing and applying new high-performance shape memory materials.

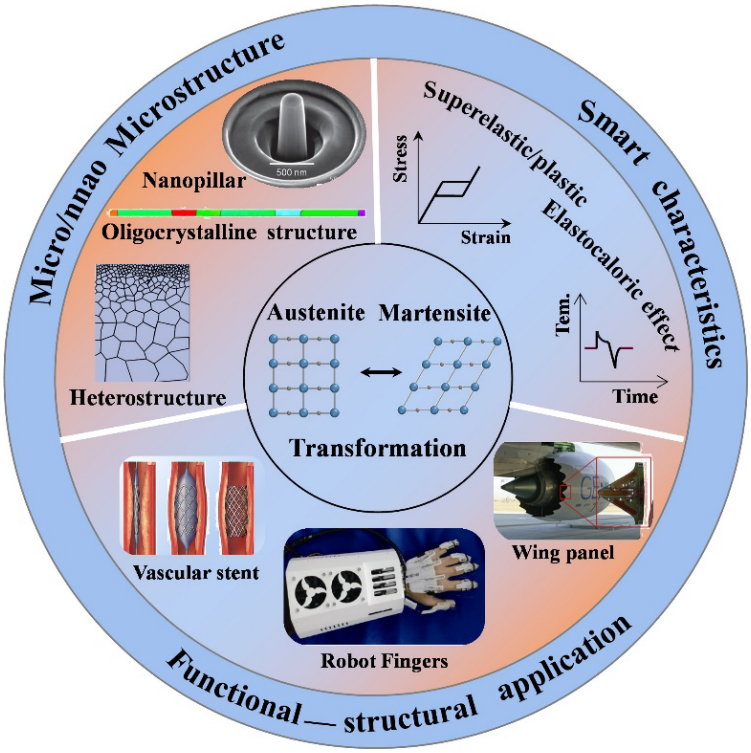

Figure 1. Characteristics and application of SMAs.

2. Overview of Superelasticity/Superplasticity Metallic Materials

Elasticity describes a material's ability to return to its original shape post-deformation, characterized by strain recoverability. Typically, most metals exhibit elastic strains of ~0.2%. Superelasticity describes the capacity of certain alloys to undergo substantial deformation at room temperature and fully recover their original shape upon unloading. This phenomenon is also termed pseudoelasticity. In contrast, superplasticity is the ability of a material to achieve exceptionally high tensile elongations under specific thermomechanical conditions, such as high temperature and a controlled strain rate. This property is particularly advantageous for the processing and forming of complex components, including those made from SMAs. Superplasticity is a characteristic of fine-grained materials, achieved within a specific temperature range and under a controlled strain rate. In contrast, superelasticity describes a material's capacity to undergo large, recoverable nonlinear strains upon unloading. This behavior is temperature-dependent and originates from a reversible, stress-induced martensitic phase transformation. The energy dissipation inherent to this transformation results in a hysteresis loop in the stress-strain curve.

Nitinol (NiTi) is the most commercially successful shape memory alloy, combining excellent superelasticity and shape memory effect. It has the advantages of high recoverable strain, excellent biocompatibility, and adjustable phase transition temperature. The limited functional fatigue life of these materials under cyclic loading, caused by the accumulation of residual deformation and dislocation activity, constrains their broader practical application. An in-depth investigation of functional fatigue's microscopic mechanisms and the correlation between microstructure and the degradation of macroscopic properties is crucial for predicting the service life of alloys and enhancing their reliability.

Gum Metal is a type of β-Ti alloy with excellent mechanical properties, close to the theoretical strength limit, and can undergo significant plastic deformation in the absence of conventional dislocation activity. The unique

deformation mechanism may involve dislocation-free plasticity. Simultaneously achieving an optimal combination of ultra-high strength, a low elastic modulus, superelasticity, and a near-absence of work hardening remains exceptionally challenging. Furthermore, the high cost of noble alloying elements (e.g., Ta, Nb, Hf) and the complexity of the preparation process significantly constrain widespread adoption.

NiMn-based SMAs form modulated martensite structures: five-layer (5M, pseudo-tetragonal), seven-layer (7M, pseudo-orthorhombic), or non-modulated (NM, tetragonal). Among these, the NM structure exhibits greater stability and superior superelasticity based on current report. Fe-based alloys undergo transformations between FCC austenite and martensite (HCP or BCC/BCT structures), where precipitation phases and nanotwins enable thermoelastic martensitic transformation for superelasticity. However, NiMn-based SMAs are often limited by high brittleness at room temperature and associated difficulties in processing and forming. Overcoming these limitations is critical for expanding their engineering applications. The phase transitions and functional behaviors of SMAss are governed by multiple coupling factors, such as temperature, stress, and, in the case of magnetic shape memory alloys, magnetic fields. But the phase transition kinetics, deformation mechanisms, and accurate constitutive models for these materials under complex loading paths and multi-field coupling conditions remain inadequately characterized. This lack of understanding currently limits their application in high-performance actuators and sensors.

Iron-based shape memory alloys present significant cost advantages and superior machinability compared to nickel-titanium alloys. These benefits, which include lower material costs, higher strength, and greater hardness facilitate their use in large-scale applications such as civil engineering structures and automotive systems. Although iron-based alloys possess notable advantages in cost and processability, achieving stable and superior superelasticity typically necessitates a precise heat treatment regime. This requirement imposes stringent demands on production process control. The precise control of the phase transition temperature range, along with the alloy's fatigue life and its performance degradation over extended service, remains a persistent challenge.

2.1. Ni-Ti SMAs

Ni-Ti shape memory alloys (Ni-Ti SMAs) are smart materials exhibiting excellent superelasticity, shape memory effect, superior damping performance, and biocompatibility. These properties enable widespread applications in biomedicine, aerospace, and aviation. The shape memory effect, superelasticity, and fatigue resistance depend on alloy composition, grain size, crystal orientation, phase structure, and deformation methods. Both properties can be enhanced by optimizing alloy composition, fabrication processes, precipitate size, and crystallographic texture. Generally, one-dimensional nanomaterials (e.g., freestanding nanowires and pillars) exhibit higher elastic strains (4–9%) than bulk counterparts. NiTi SMAs show significant potential as elastocaloric refrigerants for solid-state cooling. They undergo an ordered transformation: from high-temperature body-centered cubic (BCC) β-phase to room-temperature CsCl-type B2 phase. During cooling, B2 phase may transform directly to monoclinic B19' martensite or via intermediate R-phase. However, bulk polycrystalline NiTi SMAs exhibit poor superelasticity and cyclic instability [29–33], significantly reducing refrigeration efficiency. Performance degradation primarily results from dislocation slip due to austenite-martensite lattice incompatibility or stress concentration at triple junctions. Dislocation generation and accumulation impede strain recovery, ultimately causing functional degradation during cycling [34–39].

Thus, enhancing functional cycling stability is crucial for engineering applications. Introducing secondary phases improves NiTi SMA cyclic stability. Ti_3Ni_4 nanoprecipitates in NiTi alloys hinder dislocation motion, effectively enhancing cyclic stability [23,24,40]. Selective laser cladding of $Ni_{50.4}Ti_{49.6}$ (at.%) produces Ti_3Ni_4 nanoprecipitates (~50 nm), enabling stable tensile recovery strains up to 3.74% after 20 loading-unloading cycles [41]. Chen et al. [26] demonstrated that cold processing and annealing of $Ni_{50.8}Ti_{49.2}$ produces 4.7% stable tensile recovery strain, attributed to nanoscale B2 grains and coherent Ti_3Ni_4 nanoprecipitates (~100 nm). Grain refinement—another performance-enhancement strategy—is widely employed. Reducing grain size impedes dislocation motion, enhancing both superelasticity and shape memory effect [42–44]. Nanostructuring metallic materials shows significant promise for enhancing mechanical properties [45]. Severe plastic deformation, including high-pressure torsion (HPT) and equal channel angular extrusion (ECAE), mitigates grain size effects on phase transformations and mechanical properties [22]. Grain refinement below 60 nm inhibits thermally induced martensitic transformation [46]. ECAE-processed $Ni_{49.7}Ti_{50.3}$ with 100–300 nm grains exhibit significantly enhanced thermal cycling stability [47].

Heterostructures—achieved through alloy design and advanced manufacturing—significantly enhance mechanical properties in brittle shape memory alloys (SMAs) compared to conventional strengthening methods [48–51]. Achieving synergistic high strength and large linear hyperelasticity depends critically on heterostructure design (Figure 2a).

Incorporating nanoscale features in austenite matrices retains martensitic cores, bypassing conventional nucleation during straining.

At the nanoscale, studies on nanocrystalline NiTi reveal different cyclic deformation mechanisms. The constrained martensitic transformation within fine grains can lead to improved functional stability due to a more reversible phase transition process, as observed via in situ techniques like X-ray diffraction and in-situ TEM [52,53]. Furthermore, microstructural engineering through methods such as precipitation, friction stir processing, or additive manufacturing can significantly enhance cyclic life [54–57]. For instance, introducing nanoscale precipitates or local chemical inhomogeneity can effectively hinder dislocation activity and manage transformation stresses, promoting a superior synergy between strength, ductility, and superelastic stability over many cycles [58–60]. Alloying elements, like Tungsten, have also been explored to improve performance.

This suppresses abrupt stress-induced martensitic transformation, promoting gradual, continuous phase transitions. Cui et al. [7] engineered a heterostructure with NiTi nanoparticles and Nb nanowires (Figure 2b,c), achieving >6% linear elastic strain and 1.6 GPa yield strength in $Ni_{41}Ti_{39}Nb_{20}$ (Figure 2d,e). Similarly, a superelastic NiTi nanocomposite [8] processed by severe plastic deformation and low-temperature annealing demonstrates 4.3% recoverable strain and 2.3 GPa yield strength. NiTi crystalline-amorphous nanocomposites (CANs) feature parallel crystalline nanolayers (~8 nm average thickness) embedded in an amorphous matrix.

In NiTi CANs, amorphous phase constraints: (1) prevent grain boundary sliding; (2) increase dislocation motion resistance; and (3) suppress nucleation/propagation of phase-transformation dislocations in nanocrystalline regions during cycling. Conversely, crystalline nanolayers impede shear band formation/propagation in the amorphous phase. NiTi CANs maintain functional stability under tensile stresses ≤1.8 GPa. This stability originates from nanocrystalline-amorphous synergy, enabling 10^8 compression cycles without failure. Additively manufactured $Ni_{515}Ti_{48.5}$ alloys develop dendritic nanocomposite microstructures. These microstructures enable 10^6 superelastic cycles in NiTi SMAs.

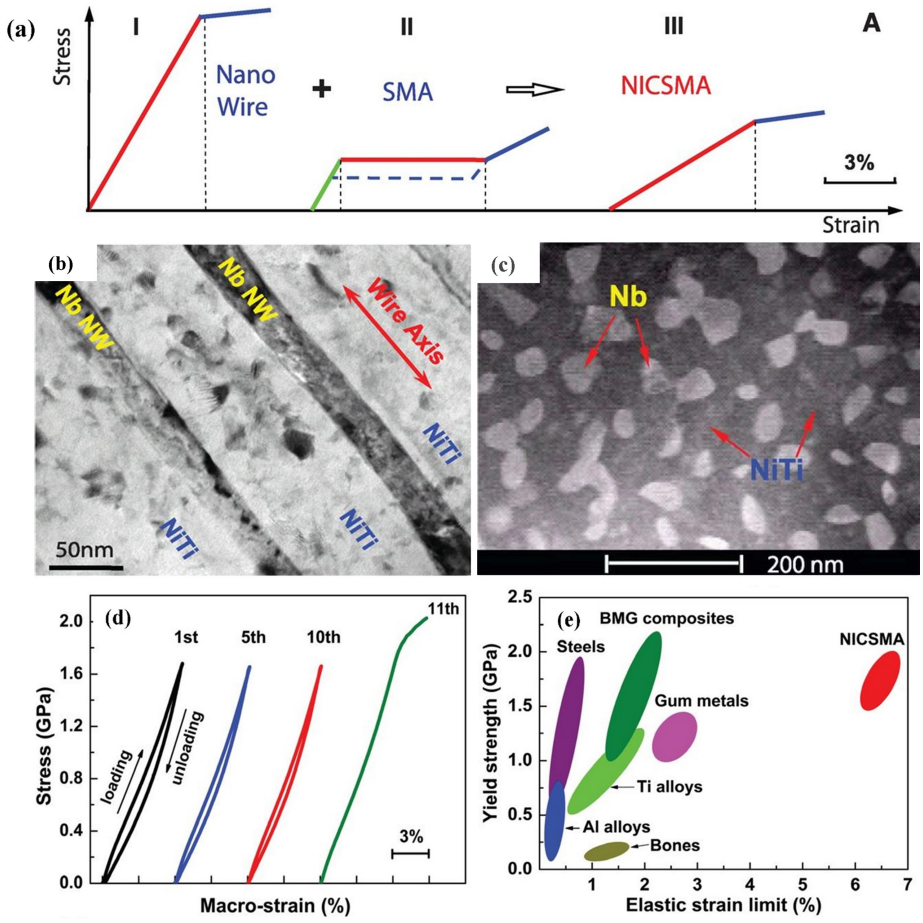

Figure 2. Schematic of NiTi nanocomposite design concept (**a**). Bright-field TEM image of $Ni_{41}Ti_{39}Nb_{20}$ nanocomposite wire (longitudinal section); (**b**) and transverse section; (**c**). Cyclic tensile stress-strain curves of $Ni_{41}Ti_{39}Nb_{20}$ nanocomposite wire at room temperature; (**d**). Yield strength vs. elastic strain limit comparison across materials; (**e**). Reproduced with permission from Reference [7]. Copyright © 2013, The American Association for the Advancement of Science.

Precipitated phases introduce additional dislocations and grain boundaries in the matrix, thus enabling strength matching. Beyond Ni- and Ti-based precipitates, precipitates from alloying elements enhance interface compatibility, fatigue resistance, and superelasticity.

2.2. Gum Metals

Gum Metal is a novel class of β-Ti alloys renowned for its unique combination of properties, including room-temperature superplasticity, an ultra-low elastic modulus, high strength following severe plastic deformation, and the Elinvar effect [61–64]. It is typically produced via arc melting or powder metallurgy, followed by thermomechanical processing and heat treatment. This processing induces significant plastic deformation, which enhances yield strength while reducing the elastic modulus. The alloy exhibits superelasticity with an elastic strain limit exceeding 2.5%, significantly higher than that of conventional metals (<1%). Its superelastic cycles are characterized by low energy dissipation and minimal hysteresis, rendering it suitable for high-precision instruments. Furthermore, its elastic modulus remains stable across a wide temperature range, making it ideal for applications in thermally fluctuating environments.

The exceptional properties of Gum Metal are achieved through precise microalloying. Saito et al. [62] demonstrated that adding elements such as Nb, Ta, V, Zr, Hf, and O to β-titanium alloys allows for the tuning of the electron/atom (e/a) ratio, bond order (Bo), and electronegativity difference ($\Delta\chi$). Jarzabek et al. [3] further proposed that controlling crystallographic orientation is key to achieving its high ductility, low elastic modulus, and high yield strength.

The superelastic mechanism in Gum Metal is attributed to a reversible stress-induced martensitic transformation, akin to traditional shape memory alloys. Notably, deformation occurs via the formation of nanoscale shear bands rather than dislocation slip, which suppresses work hardening and enables large recoverable strains [65–67].

Owing to its low elastic modulus, high strength, and excellent biocompatibility, Gum Metal is a promising material for biomedical applications such as implants, stents, and cardiovascular devices. For instance, its low Young's modulus, high resilience, and biocompatibility make it an effective orthodontic wire that provides a continuous, gentle corrective force, thereby reducing patient discomfort [68]. Its elastic modulus closely matches that of human cortical bone, which minimizes the stress-shielding effect and makes it suitable for bone transplant meshes [69,70].

In summary, Gum Metal's properties stem from its unique compositional design, nanostructural control, and reversible phase transformation mechanism. It synergistically combines a low modulus, high strength, wide temperature stability, and low energy dissipation, offering significant potential for applications in biomedicine, aerospace, and high-precision instrumentation. Future research will focus on further optimizing its composition to extend its functional temperature range, reducing production costs, and developing scalable manufacturing processes.

2.3. NiMn-Based SMAs

NiMn-based SMAs exhibit distinctive responses to external stimuli (stress, temperature, magnetic fields), enabling applications in actuators, sensors, and solid-state refrigeration [71–73]. Ni-Mn-Ga SMAs—typical Heusler alloys—exhibit outstanding superelasticity, shape memory effect, and magnetocaloric properties. Their martensitic phase transformation is diffusionless. Secondary phases can cause incomplete martensitic transformation, inducing simultaneous microcrack initiation/growth at grain boundaries and poor cyclic performance. Significant research addresses polycrystals' intrinsic brittleness and limited deformability to enhance fatigue performance Single-crystal variants eliminate internal constraints, yielding superior mechanical properties. However, single-crystal production remains time-intensive. Polycrystalline fabrication via melt spinning or Taylor-Ulitovsky methods is relatively simple and cost-effective. Triangular grain junctions typically initiate brittle cracks during deformation and limit recoverable strains. Dunand and Müullner [74] proposed matching grain size to critical sample dimensions (e.g., film thickness, wire diameter) via grain growth/shrinkage (Figure 3a). Advanced strategies like active learning are employed to optimize complex multi-component compositions for enhanced performance and stability. high-temperature actuation and large latent heat were also developed in magnetic shape memory alloy, particularly Ni-Mn-Ga-based systems [75,76]. This size effect facilitates grain-coordinated deformation, validated in fibers and foams [77,78].

Microalloying combined with size control effectively enhances NiMnGa SMA cyclic performance. The Taylor-Ulitowski method produces 5–200 μm diameter glass-coated microwires. This method reduces intergranular constraints and induces orientation, enhancing superelasticity and ductility. Xuan [25] enhanced martensite-austenite compatibility in Ni-Mn-Ga microwires via γ-nanoprecipitates from Fe/Cu doping. Oligocrystalline microstructures

enable multi-step superelasticity comparable to Ni-Mn-Ga-Co-Cu (Figures 3b,c). Taylor-method microwires develop bamboo-like structures. During loading, γ-precipitates generate elastic incompatibility stress, relaxed via reversible twinning during unloading. Ding [79] achieved >10% fully recoverable strain and multi-step superelasticity in near-<001> oriented oligocrystalline microwires. Co/Cu addition increases Ni-Mn-Ga transformation temperatures, enabling room-temperature austenite → martensite transition. This transformation remains temperature-drivable (Figure 3d,e).

Oligocrystalline structures enable polycrystalline alloys to approach single-crystal properties.Free surfaces in these structures reduce grain-boundary constraints, facilitating coordinated intergranular deformation. This approach extends to other SMAs including microfilaments and porous foams and porous foams [79–81]. High-temperature annealing optimizes the structure and magnetic properties of Ni-Mn-Ga-based glass-coated microwires, while novel composition design, as in Ni-Mn-Ga-Co-Cu alloys, enables giant high-temperature superelasticity, highlighting key strategies for enhancing their high-temperature functional performance [82,83]. Ueland [84] demonstrated Cu-Al-Zn oligocrystalline microwires with two-order fatigue life improvement versus conventional alloys. Chen [85] similarly fabricated Ni-Mn-Fe-Ga microwires with an oligocrystalline structure and a large recoverable strain of up to 15% and stable superelasticity after 1200 cycles. When combined with favorable grain orientation, oligocrystalline structures suppress intergranular fracture while enhancing superelasticity and fatigue performance. Microalloying and size control produce oligocrystalline structures and nanoprecipitates that enhance lattice compatibility, superelasticity, and functional stability in Ni-Mn-Ga SMAs. These advances enable device miniaturization and intelligent system development, demonstrating significant scientific and engineering value.

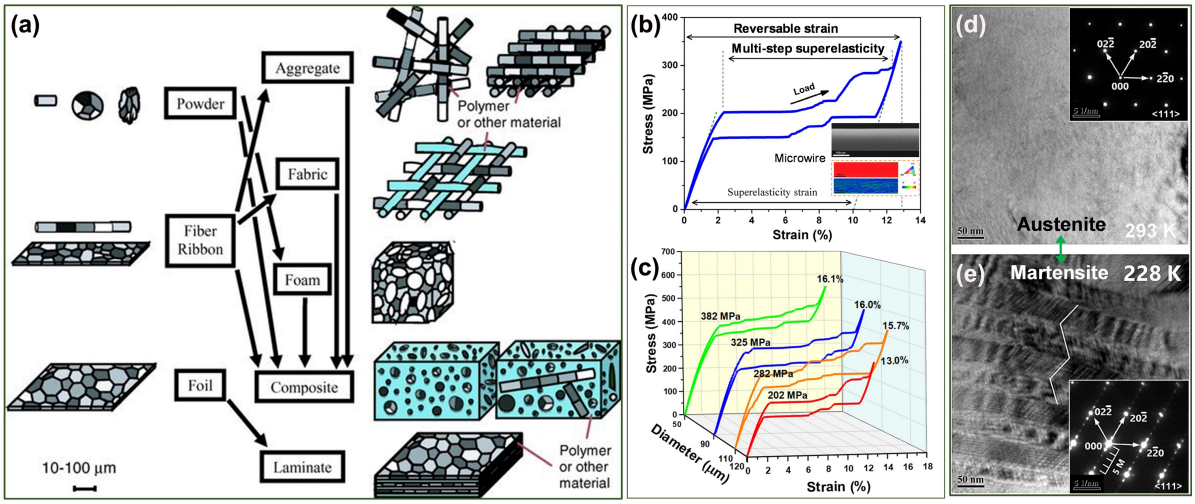

Figure 3. Size effect of NiMn-based SMAs superelasticity. Reproduced with permission from Reference [65]. Copyright 2011, The John Wiley and Sons. (**a**). Uniaxial tensile stress-strain curve of NiMnGaCoCu alloy at 300 K; (**b**). Stress-strain curves of microwires with different diameters at 573 K. Reproduced with permission from Reference [25]. Copyright 2021, Elsevier; (**c**). Diffraction spots of austenite at 293 K; (**d**). Diffraction spots of martensite at 228 K; (**e**). Reproduced with permission from Reference [79]. Copyright 2017, Elsevier.

2.4. Fe-Based SMAs

Fe-based SMAs offer unique advantages including high strength, superplasticity, favorable shape memory characteristics, and low cost. However, most undergo non-thermoelastic martensitic transformations, preventing superelasticity. Thermoelastic behavior can be induced through precipitation phases and nanotwins, enabling reversible FCC austenite to BCC/HCP martensite transformations (Figure 4). These alloys maintain remarkable performance under extreme service conditions, enabling applications as heavy machinery track fishplates, seismic dampers, and rail couplers in material-intensive systems [86]. Achieving room-temperature superelasticity in Fe-based SMAs remains challenging, though aging-induced nanoscale precipitates facilitate reversible martensitic transformation, enhancing superelasticity [87]. A breakthrough occurred in polycrystalline FeNiCoAlTaB, achieving 13.5% superelastic strain [12], resulting from synergistic coherent nanoprecipitates and large grain size. Similarly, Fe-Mn-Al-Ni achieves >5% superplastic strain at room temperature via nanoprecipitation [28]. Both systems generate high local stresses and anisotropy at grain boundaries during transformation, promoting brittle fracture and superelasticity suppression. Reducing grain-boundary constraints promotes coordinated intergranular deformation, effectively enhancing superplasticity.

The cyclic performance of Fe-based shape memory alloys is critically linked to microstructural control. Strategies like promoting abnormal grain growth and specific crystallographic orientations, studied via in-situ techniques, are key to enhancing superelastic stability by minimizing energy dissipation at grain boundaries [88–90]. Zhao et al. [91] achieved 6% recoverable strain in directionally solidified $Fe_{34}Mn_{15}Al_{7.5}Ni_{1.5}Co$ via directional solidification (DS), inducing >20 mm abnormal grain growth. This suppresses grain-boundary constraints, weakening martensitic transformation resistance. These strategies lower transformation resistance, enhancing reversible strain. However, cyclic degradation remains a significant challenge, directly impacting functional fatigue and the seismic performance of applications [92]. Advanced manufacturing and processing methods, such as wire-arc additive manufacturing and high-pressure torsion, are being explored to engineer refined and textured microstructures that aim to improve both functional and structural stability under repeated loading [93].

Temperature-dependent critical stress represents another key feature of martensitic transformations. Alloying with temperature-invariant elements effectively mitigates this limitation. Cr doping alters critical stress temperature dependence above 50 K without increasing strain hysteresis in Fe-Mn-Al-Cr-Ni single crystals [13]. B2-structured precipitates with irregular stacking sequences induce matrix distortion during thermoelastic martensitic transformation. While NiMn-based alloys exhibit temperature-unstable superelasticity, $Fe_{34}Mn_{13.5}Al_3Cr_{7.5}Ni$ single crystals maintain near-constant superelastic strain from 10–300 K, achieving 3.5% recoverable strain (Figure 5a,b). This temperature-stable superelasticity arises from synergistic temperature-invariant elements and precipitate formation.For Fe-based alloys, processing facilitates transitioning from plastic deformation to shape memory behavior [94–96]. Recent targeted design strategies enhance Fe-based SMA superelasticity through: (1) matrix strengthening via coherent nanoprecipitates; (2) favorable orientation creation; and (3) grain-boundary constraint reduction. Abnormal grain growth in α single-phase or α + γ two-phase regions produces grains exceeding sample dimensions, reducing grain-boundary constraints and enhancing superelasticity

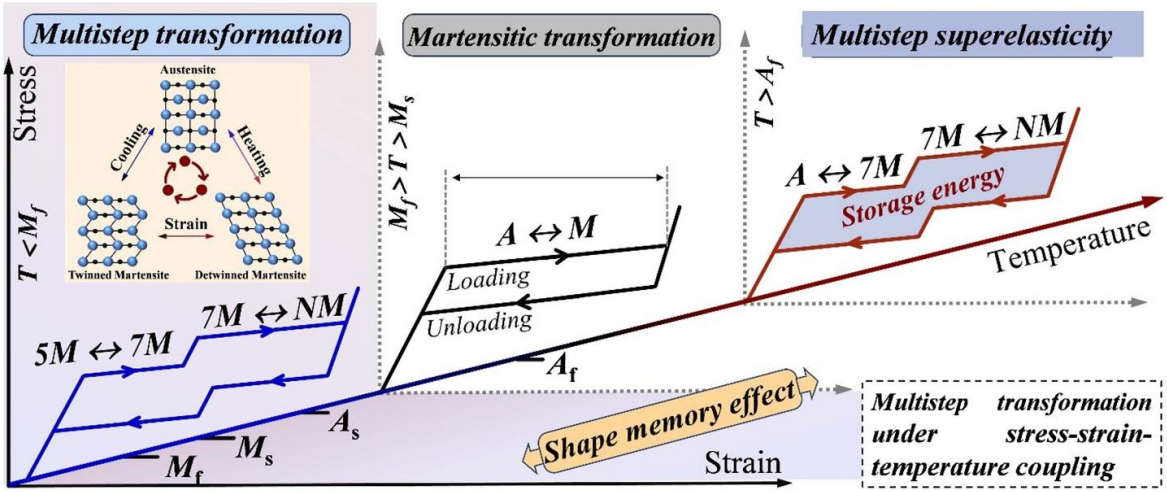

Figure 4. Multi-step transformation of SMAs under stress–strain–temperature coupling. Reproduced with permission from Reference [94]. Copyright 2025, IOP Publishing Ltd. [90].

However, fatigue failure in Fe-based SMAs under cyclic loading primarily results from obstructed reversible martensitic transformation, leading to residual strain accumulation [97]. Research on Fe-based SMA cyclic stability remains limited. Figure 6 compares cyclic stability across SMA types, revealing lower functional stability in Fe-based SMAs versus NiMn- and NiTi-based counterparts. Improving cyclic stability requires minimizing martensite interface pinning and residual strain accumulation during phase cycling. Guided reversible movement along specific lattice pathways enables early defect elimination, stabilizing energy dissipation during transformations. Dispersed nanoprecipitates induce back stress on martensite laths, facilitating interface movement along specific parent-phase/ε-martensite pathways. Prestressing synergistically enhances ε-martensite formation through increased stacking fault generation, while reverse transformation occurs during unloading. Stress-induced ε-martensite forms and decomposes during repeated tensile-compressive cycling.

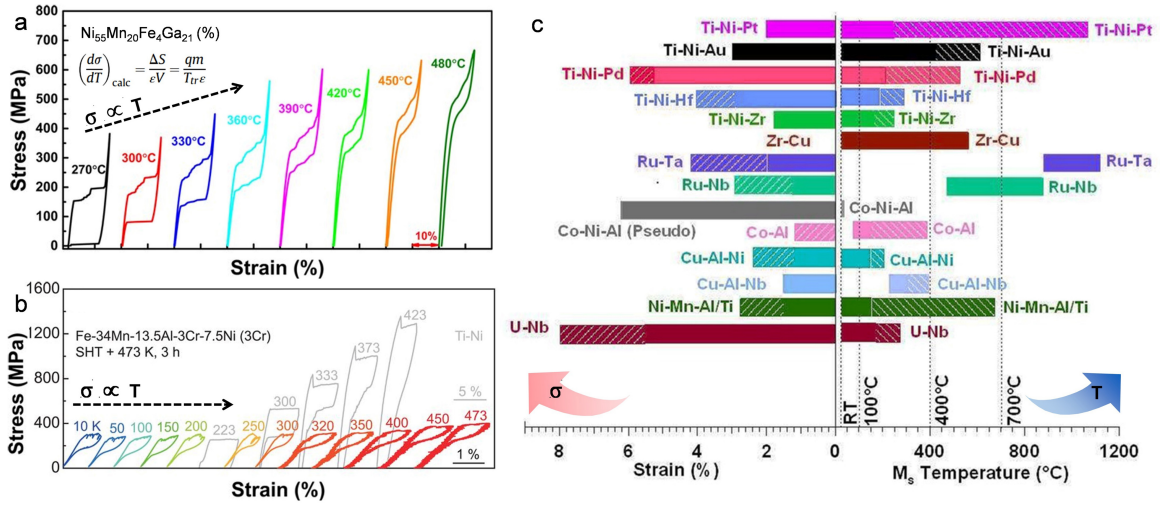

Figure 5. Stress-strain curves of $Ni_{55}Mn_{20}Fe_4Ga_{21}$ in different temperature ranges (**a**). Reproduced with permission from Reference [85]. Copyright © 2022, The Author(s). Comparison of stress-strain curves between $Fe_{36}Mn_{11}Al_{7.5}Cr_3Ni$ and NiTi in different temperature ranges; (**b**). Reproduced with permission from Reference [13]. Copyright © 2020, The American Association for the Advancement of Science.

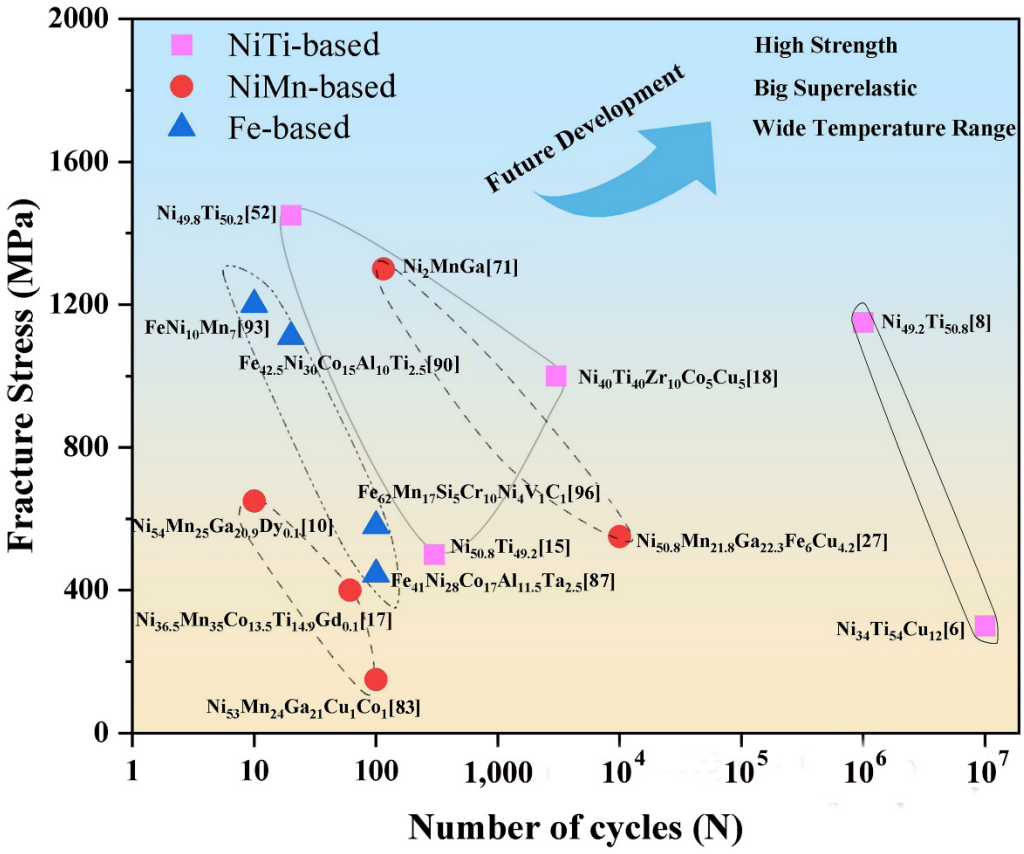

Figure 6. Comparison of cyclic stability of various types of SMAs at room temperature.

This repetitive transformation reduces cyclic-loading-induced stress concentrations, inhibits local dislocation accumulation, and suppresses fatigue crack initiation/propagation. Sufficient slip resistance at manageable transformation stresses reduces plasticity at martensite-austenite interfaces. Functional stability in Fe-based SMAs is achieved through synergistic structural design and precipitation control. Fe-based SMAs exhibit high superelasticity and functional stability across wide temperature ranges, showing strong potential for high-damping and sensor applications. This enables deployment in extreme environments (e.g., lunar/Martian infrastructure), supporting aerospace and large-scale seismic engineering projects.

2.5. Comparison of the Structural-Functional Integrated Materials

Superior mechanical properties enable multifunctional performance in shape memory alloys. NiTi-based SMAs exhibit distinctive properties including unique functionality, biocompatibility, and damping characteristics [54–56]. Their ultrahigh strength—derived from nanowire mechanical properties—enables deployment in demanding smart devices. NiTi's exceptional functional stability makes it particularly attractive among SMAs. NiMn-based SMAs uniquely exhibit magnetic shape memory, generating macroscopic strains through magnetic-field-driven martensitic variant rearrangement [98–100]. Ni-Mn-Ga single crystals achieve >10% magnetic-field-induced strain in martensitic phase, enabling actuator, sensor, and energy harvester design [101,102]. Phase transformations (stress/magnetic-field-driven) involve heat exchange via elastocaloric [103] or magnetocaloric [104] effects, as demonstrated in NiMnCo(Sn,In) alloys [105–108]. Enhanced superelasticity in NiMn-based SMAs provides foundational support for multifunctional implementation.

Fe-based superelastic SMAs exhibit essential properties: high strength, large strain, and superelasticity [12,28,86,87]. Newly developed Fe-Mn-Al-Cr-Ni alloys show controllable critical-stress temperature dependence (10–300 K) via Cr optimization, enabling precision metrology applications by mitigating thermal expansion. Their lower cost and superior cold-workability facilitate use as advanced structural-functional integrated materials [109,110]. Finally, the basic properties of the four types of materials are summarized in Table 1.

Table 1. Comparison of general characteristics of NiTi-based, Gum Metal, NiMn-based and Iron-based SMA.

Characteristics	NiTi-Based	NiMn-Based	Gum Metal	Iron-Based
Superelasticity	Excellent (~8%), stability	Moderate (usually < 5%), Magnetic fields	Excellent (recovery strain 2.5–3.5%), nonlinear elasticity	Poor (usually < 3%), recovery, stability
Superplasticity	High temperature superplasticity for hot forming	High temperature superplasticity	Superplastic forming, large deformation cold working at room temperature.	Wide temperature range superplasticity
Shape memory effect	Excellent (large recovery strain, fast driving speed, long life)	Excellent (low strain and force), Driven by magnetic field (rather than thermally)	None (superelasticity only, no thermally induced shape memory effect)	Medium (recovery strain 3–4%), low cost, but poor fatigue performance
Mechanism	Thermoelastic martensitic transformation induced by stress or temperature	Magnetoelastic martensitic transformation (MFIT or reorientation)	Dislocation-free/nanoscale mechanism (reversible nanoscale shear in β-titanium alloys)	Non-thermoelastic martensitic transformation
Drive mode	Thermal (temperature change), stress.	Magnetic	Stress (loading/unloading).	Thermal (temperature change)
Elastic modulus	Soft (30–80 GPa)	Depending on composition.	Medium (40–60 GPa), close to human bone.	High (150–200 GPa)
Strength	High (tensile strength can reach over 1 GPa).	High.	Ultra-high (tensile strength can reach 1.5–2.0 GPa).	Medium
Cost	High (contains Ni and Ti, difficult to smelt and process).	Very high (contains precious metals such as Ga).	Very high (contains Ta, Zr, Nb, etc., extremely difficult to smelt and process).	Very low (primarily Fe, easy to industrialize).
Main Features	Good biocompatibility, stable performance, long fatigue life. Widely used.	Fast, non-contact magnetic drive with high response frequency. High-frequency drives.	"Super" metal, combining low modulus, ultra-high strength, ultra-large elastic strain, and cold formability.	Extremely low cost, suitable for non-precision fields such as large-scale civil engineering

MFIT—Magnetic field-induced transformation.

3. Prospects and Conclusions

3.1. Prospect

Future research on SMAs is anticipated to progress along several critical avenues:

(1) Design of new high-Performance smart materials.

Advanced methods such as high-throughput computing and machine learning will significantly improve the efficiency of developing new shape memory materials. Key areas include developing high-temperature shape memory alloy systems, as well as cost-effective iron- and copper-based alloy systems. Multi-element alloying strategies, such as the addition of elements such as Cu, Nb, or Hf to NiTi alloys, will continue to be important approaches for optimizing phase transition temperature, hysteresis, and fatigue performance.

(2) Advanced fabrication and processing technologies.

Additive manufacturing (such as 3D/4D printing) enables near-net-shape fabrication of complex parts and enhances material properties by precisely controlling process parameters to manipulate microstructure.

(3) Integrated structural-functional design.

Combining topology optimization, gradient material design, and intelligent control algorithms can optimize the macroscopic performance of shape memory alloy devices. In the aerospace field, intelligent structures such as deformable wings and adaptive engine inlets are expected to significantly improve aircraft aerodynamic performance and energy efficiency.

(4) Multidisciplinary application expansion.

SMAs will further integrate with cutting-edge fields such as biomedical engineering, micro-nanosystems, and soft robotics. For example, magnetically controlled NiTi microgrippers can be used for cell manipulation in micromanipulation, while biodegradable Fe- and Mg-based shape memory alloys are expected to achieve significant breakthroughs in medical applications as temporary implant materials.

(5) In-depth research on fundamental theory.

Relying on advanced characterization techniques (such as in situ electron microscopy and synchrotron X-ray diffraction) and multi-scale simulation methods, future research will focus on revealing the microscopic mechanisms of phase transformation and the motion patterns of martensitic variant interfaces. In particular, the crystal structure analysis of modulated martensite in Ni-Mn-based alloys will deepen our understanding of the physical nature of its magnetic-thermal-mechanical coupling behavior and provide theoretical support for material design.

3.2. Conclusions

This article systematically reviews recent research progress in superelastic and superplastic shape memory alloys (SMAs), with a focus on the properties and application prospects of major systems, including NiTi-based, NiMn-based, Fe-based, and Cu-based alloys. Owing to their unique shape memory effect and superelasticity, SMAs have demonstrated significant application potential in fields such as aerospace, biomedicine, automotive engineering, and smart structures.

NiTi-based alloys remain the most comprehensively performing SMAs, with their properties continually enhanced through multi-component alloying and advanced processing techniques. NiMn-based ferromagnetic shape memory alloys (FSMAs) enable magnetic field control, rendering them highly promising for applications in magnetic actuation and refrigeration. Owing to their cost-effectiveness, Fe- and Cu-based alloys are strong candidates for large-scale engineering applications. Novel titanium-based alloys such as Gum Metal provide new insights for designing superelastic materials.

The exploration of high-temperature, low-cost, and lightweight shape memory alloys, alongside novel materials exhibiting multi-shape memory and two-way memory effects, constitutes a key future research direction. For mature alloy systems, deeper collaboration will be pursued with fields including biomedicine, micro-nano electromechanical systems, soft robotics, and artificial intelligence to explore novel principles and applications. Future SMA research will advance toward enhancing performance, reducing cost, and integrating structural and functional properties for diversified applications. Through material innovation, process optimization, theoretical advances, and multidisciplinary integration, SMAs are poised to play a key role in an expanding range of fields by serving as core functional materials for smart structural systems and advanced equipment.

Author Contributions

C.P.: writing—original draft, writing—review & editing; H.L.: visualization; K.Z.: comments; A.C.: conceptualization; Z.D.: supervision, writing—review & editing; F.L.: formal analysis, investigation; A.L.: Validation. All authors have read and agreed to the published version of the manuscript.

Funding

This research was funded by the National Natural Science Foundation of China (Grant Nos. 51771121 and 52303091), the Science and Technology Commission of Shanghai Municipality (Grant No. 25ZR1401258), the Shanghai Yangfan Program (Grant No. 22YF1430200), and the Shanghai Yangpu District Medical Key Discipline Construction Fund (Grant No. 22YPZA08).

Institutional Review Board Statement

This review was written and compiled based on public data. It does not involve any human-related clinical trials. Therefore, no application was submitted to the ethical review committee of the relevant institution.

Informed Consent Statement

Not applicable.

Data Availability Statement

The data of this study are available upon reasonable request from the authors.

Conflicts of Interest

The authors declare no conflict of interest.

References

1. Lu, K. Making strong nanomaterials ductile with gradients. *Science* **2014**, *345*, 1455–1456.
2. Ma, E.; Zhu, T. Towards strength–ductility synergy through the design of heterogeneous nanostructures in metals. *Mater. Today* **2017**, *20*, 323–331.
3. Ovid'Ko, I.A.; Valiev, R.Z.; Zhu, Y.T. Review on superior strength and enhanced ductility of metallic nanomaterials. *Prog. Mater. Sci.* **2018**, *94*, 462–540.
4. Li, X.T.; Liu, R.; Hou, J.P.; et al. Trade-off model for strength-ductility relationship of metallic materials. *Acta Mater.* **2025**, *289*, 120942.
5. Meyers, M.; Mishra, A.; Benson, D.; et al. Mechanical properties of nanocrystalline materials. *Prog. Mater. Sci.* **2005**, *51*, 427–556.
6. Christoph, C.B.; Ge, W.W.; Li, M.M.; et al. Ultralow-fatigue shape memory alloy films. *Science* **2015**, *348*, 1004–1007.
7. Hao, S.; Cui, L.; Jiang, D.; et al. A Transforming Metal Nanocomposite with Large Elastic Strain, Low Modulus, and High Strength. *Science* **2013**, *339*, 1191–1194.
8. Hua, P.; Xia, M.L.; Onuki, Y.; et al. Nanocomposite NiTi shape memory alloy with high strength and fatigue resistance. *Nat. Nanotechnol.* **2021**, *16*, 409–413.
9. Mahsa, N.; Ville, L.; Alexei, S.; et al. Effects of 1 at.% additions of Co, Fe, Cu, and Cr on the properties of Ni-Mn-Ga-based magnetic shape memory alloys. *Scr. Mater.* **2023**, *224*, 115116.
10. Tong, W.; Liang, L.; Xu, J.; et al. Achieving enhanced mechanical, pseudoelastic and elastocaloric properties in Ni-Mn-Ga alloys via Dy micro-alloying and isothermal mechanical cyclic training. *Scr. Mater.* **2022**, *209*, 114393.
11. Jia, Z.; Chen, Z.; Zhang, Y.; et al. Huge high-temperature superelasticity and complete strains recovery above 773 K in Ni–Mn–Ga-based microwire. *Appl. Phys. Lett.* 2025, 126. https://doi.org/10.1063/5.0267990.
12. Tanaka, Y.; Himuro, Y.; Kainuma, R.; et al. Ferrous Polycrystalline Shape-Memory Alloy Showing Huge Superelasticity. *Science* **2010**, *327*, 1488–1490.
13. Xia, J.; Noguchi, Y.; Kainuma, R.; et al. Iron-based superelastic alloys with near-constant critical stress temperature dependence. *Science* **2020**, *369*, 855–858.
14. Beihai, H.; Bo, X.; Sen, T.; et al. Effect of aspect ratio on the elastocaloric effect and its cyclic stability of nanocrystalline NiTi shape memory alloy. *J. Mater. Res. Technol.* **2023**, *25*, 6288–6302.
15. Xu, F.; Zhu, C.; Wang, J.; et al. Enhanced elastocaloric effect and mechanical properties of Gd-doped Ni-Co-Mn-Ti-Gd metamagnetic shape memory alloys. *J. Alloys Compd.* **2023**, *960*, 170768.
16. Lu, N.H.; Chen, C.H. Improving the functional stability of TiNi-based shape memory alloy by multi-principal element design. *Mater. Sci.Eng. A* **2023**, *872*, 144999.
17. Cheng, F.; Qiu, C.X.; Zheng, Y.; et al. Shape Memory Alloys for Civil Engineering. *Materials* **2023**, *16*, 787.
18. Dornelas, V.D.; Oliveira, A.S.; Savi, M.; et al. Fatigue on shape memory alloys: Experimental observations and constitutive modeling. *Int. J. Solids Struct.* **2020**, *213*, 1–24.
19. Norfleet, D.M.; Sarosi, P.M.; Manchiraju, S.; et al. Transformation-induced plasticity during pseudoelastic deformation in Ni–Ti microcrystals. *Acta Mater.* **2009**, *57*, 3549–3561.
20. Ahadi, A.; Ghorabaei, A.S.; Shirazi, H.; et al. Bulk NiTiCuCo shape memory alloys with ultra-high thermal and superelastic cyclic stability. *Scr. Mater.* **2021**, *200*, 113899.
21. Shahmir, H.; Nili-Ahmadabadi, M.; Huang, Y.; et al. Shape memory characteristics of a nanocrystalline TiNi alloy processed by HPT followed by post-deformation annealing. *Mater. Sci. Eng. A* **2018**, *734*, 445–452.
22. Li, Z.H.; Xiang, G.Q.; Cheng, X.H.; et al. Effects of ECAE process on microstructure and transformation behavior of TiNi shape memory alloy. *Mater. Des.* **2006**, *27*, 324–328.
23. Sidharth, R.; Celebi, T.B.; Sehitoglu, H. Origins of functional fatigue and reversible transformation of precipitates in NiTi shape memory alloy. *Acta Mater.* **2024**, *274*, 119990.
24. Timofeeva, E.E.; Panchenko, E.Y.; Zherdev, M.V.; et al. Effect of one family of Ti_3Ni_4 precipitates on shape memory effect, superelasticity and strength properties of the B_2 phase in high-nickel [001]-oriented Ti-51.5 at.%Ni single crystals. *Mater. Sci. Eng. A* **2022**, *832*, 142420.

25. Xuan, J.M.; Gao, J.J.; Ding, Z.Y.; et al. Improved superelasticity and fatigue resistance in nano-precipitate strengthened $Ni_{50}Mn_{23}Ga_{22}Fe_4Cu_1$ microwire. *J. Alloys Compd.* **2021**, *877*, 160296.
26. Sobrero, C.; Lauhoff, C.; Langenkämper, D.; et al. Impact of test temperature on functional degradation in Fe-Ni-Co-Al-Ta shape memory alloy single crystals. *Mater. Lett.* **2021**, *291*, 129430.
27. Villa, E.; D'Eril, M.M.; Nespoli, A.; et al. The role of γ-phase on the thermo-mechanical properties of NiMnGaFe alloys polycrystalline samples. *J. Alloys Compd.* **2018**, *763*, 883–890.
28. Omori, T.; Ando, K.; Okano, M.; et al. Superelastic Effect in Polycrystalline Ferrous Alloys. *Science* **2011**, *333*, 68–71.
29. Hong, H.; Gencturk, B.; Saiidi, M.S. Material characterization of iron-based shape memory alloys for use in self-centering columns. *Smart Mater. Struct.* **2024**, *33,* 075001.
30. Choi, W.S.; Pang, E.I.; Ko, W.S.; et al. Orientation-dependent plastic deformation mechanisms and competition with stress-induced phase transformation in microscale NiTi. *Acta Mater.* **2021**, *208*, 116731.
31. Li, Q.; Chen, Y.; Liu, Y.; et al. Non-linear temperature dependences of pseudoelastic stress and stress hysteresis of a nanocrystalline $Ni_{47}Ti_{50}Fe_3$ alloy. *Acta Mater.* **2024**, *265*, 119625.
32. Li, R.; Liaw, P.K.; Jiang, J.; et al. Advanced Applications for Smart-Metallic Materials. *Smart Mater. Devices* **2025**, *1*, 1.
33. Wang, X.B.; Kustov, S.; Li, K.; et al. Effect of nanoprecipitates on the transformation behavior and functional properties of a Ti50.8 at.% Ni alloy with micron-sized grains. *Acta Mater.* **2015**, *82*, 224–233.
34. Lu, H.Z.; Liu, L.H.; Yang, C.; et al. Simultaneous enhancement of mechanical and shape memory properties by heat-treatment homogenization of Ti_2Ni precipitates in TiNi shape memory alloy fabricated by selective laser melting. *J. Mater. Sci. Technol.* **2022**, *101*, 205–216.
35. Xu, B.; Wang, C.; Wang, Q.Y.; et al. Toward tunable shape memory effect of NiTi alloy by grain size engineering: A phase field study. *J. Mater. Sci. Technol.* **2024**, *168*, 276–289.
36. Chaithany, K.N.; Pagare, A.; Brokmeier, H.G.; et al. Transformation textures in Ni rich NiTi shape memory alloy. *Mater. Sci. Eng. A* **2022**, *835*, 142594.
37. Chumlyakov, Y.I.; Kireev, I.V.; Vyrodova, A.V.; et al. Effect of marforming on superelasticity and shape memory effect of [001]-oriented $Ni_{50.3}Ti_{49.7}$ alloy single crystals under compression. *J. Alloys Compd.* **2022**, *896*, 162841.
38. Zu, X.; Wen, H.; Peng, Z.; et al. Enhanced Functional Fatigue Resistance of Cu-Al-Mn Superelastic Wire Bamboo-Like Grain Structure. *Fatigue Fract. Eng. Mater. Struct.* **2025**, *48*, 1248–1260.
39. Sehitoglu, H.; Wu, Y.; Ertekin, E.; et al. Elastocaloric effects in the extreme. *Scr. Mater.* **2018**, *148*, 122–126.
40. Sedmák, P.; Šittner, P.; Pilch, J.; et al. Instability of cyclic superelastic deformation of NiTi investigated by synchrotron *X*-ray diffraction. *Acta Mater.* **2015**, *94*, 257–270.
41. Ryu, H.; Lee, Z.F.; Kim, J.Y.; et al. Cyclic stability in NiTi and NiTiCu thin films: Role of precipitates in low-and high-cycle regimes. *Scr. Mater.* **2024**, *250*, 116189.
42. Chen, H.; Xiao, F.; Liang, X.; et al. Stable and large superelasticity and elastocaloric effect in nanocrystalline Ti-44Ni-5Cu-1Al (at%) alloy. *Acta Mater.* **2018**, *158*, 330–339.
43. Battaglia, M.; Sellitto, A.; Giamundo, A.; et al. Advanced material thermomechanical modelling of shape memory alloys applied to automotive design. *Shape Mem. Superelasticity* **2024**, *10*, 297–313.
44. Wu, Y.; Ertekin, E.; Sehitoglu, H.; et al. Elastocaloric cooling capacity of shape memory alloys—Role of deformation temperatures, mechanical cycling, stress hysteresis and inhomogeneity of transformation. *Acta Mater.* **2017**, *135*, 158–176.
45. Li, X.; Liang, Q.; Dong, T.; et al. Fatigue-resistant elastocaloric effect in hypoeutectic $TiNi_{58}$ alloy with heterogeneous microstructure. *Acta Mater.* 2024, 262,119464.
46. Tong, Y.X.; Shuitcev, A.; Zheng, Y.F.; et al. Development of TiNi-based shape memory slloys with high cycle stability and high transformation temperature. *Adv. Eng. Mater.* **2020**, *22*, 1900496.
47. Cui, J.; Chu, Y.S.; Famodu, O.O.; et al. Combinatorial search of thermoelastic shape-memory alloys with extremely small hysteresis width. *Nat. Mater.* **2006**, *5*, 286–290.
48. Xue, D.Q.; Li, Z.H.; Pan, Y.; et al. Low hysteresis and high cyclic stability in a $Ti_{50}Ni_{45.2}Cu_1Fe_{3.8}$ shape memory alloy. *J. Alloys Compd.* **2023**, *955*, 170188.
49. Kockar, B.; Karaman, I.; Kim, J.I.; et al. A method to enhance cyclic reversibility of NiTiHf high temperature shape memory alloys. *Scr. Mater.* **2006**, *54*, 2203–2208.
50. Lua, H.Z.; Ma, H.W.; Cai, W.S.; et al. Stable tensile recovery strain induced by a Ni_4Ti_3 nanoprecipitate in a $Ni_{50.4}Ti_{49.6}$ shape memory alloy fabricated via selective laser melting. *Acta Mater.* **2021**, *219*, 117261.
51. Peng, C.; Liu, Y.F.; Min, N.; et al. Enhanced two-way shape memory effect in nanocrystalline NiTi shape memory alloy wires. *Scr. Mater.* **2023**, *236*, 115669.
52. Ahadi, A.; Sun, Q. Stress-induced nanoscale phase transition in superelastic NiTi by *in situ X*-ray diffraction. *Acta Mater.* **2015**, *90*, 272–281.
53. Li, Z.; Cai, J.; Zhao, Z.; et al. Local chemical inhomogeneity enables superior strength-ductility-superelasticity synergy in additively manufactured NiTi shape memory alloys. *Nat. Commun.* **2025**, *16*, 1941.

54. Surikov, N.Y.; Panchenko, E.; Chumlyakov, Y.I.; et al. Cyclic stability of the elastocaloric effect in heterophase [001]-oriented TiNi single crystals. *Appl. Phys. Lett.* **2024**, *125*, 151901.
55. Tobushi, H.; Iwanaga, H.; Tanaka, K.; et al. Deformation behaviour of TiNi shape memory alloy subjected to variable stress and temperature. *Contin. Mech. Thermodyn.* **1991**, *3*, 79–93.
56. Dao, M.; Lu, L.; Asaro, R.J.; et al. Toward a quantitative understanding of mechanical behavior of nanocrystalline metals. *Acta Mater.* **2007**, *55*, 4041–4065.
57. Tyc, O.; Iaparova, E.; Molnárová; O; et al. Stress induced martensitic transformation in NiTi at elevated temperatures: Martensite variant microstructures, recoverable strains and plastic strains. *Acta Mater.* **2024**, *279*, 120287.
58. Toghani-Taheri, F.; Khodabakhshi, F.; Malekan, M.; et al. Cyclic pseudoelastic behavior of friction stir processed NiTi shape memory alloy: Microstructure and W-alloying. *Mater. Sci. Eng. A* **2025**, *927*,148000.
59. Waitz, T.; Kazykhanov, V.; Karnthaler, H.P.; et al. Martensitic phase transformations in nanocrystalline NiTi studied by TEM. *Acta Mater.* **2003**, *52*, 137–147.
60. Gall, K.; Maier, H.J. Cyclic deformation mechanisms in precipitated NiTi shape memory alloys. *Acta Mater.* **2002**, *50*, 4643–4657.
61. He, Q.F.; Wang, J.G.; Chen, H.A.; et al. A highly distorted ultraelastic chemically complex Elinvar alloy. *Nature* **2022**, *602*, 251–257.
62. Saito, T.; Furuta, T.; Hwang, J.H.; et al. Multifunctional alloys obtained via a dislocation-free plastic deformation mechanism. *Science* **2003**, *300*, 464–467.
63. Jarząbek, D.M.; Włoczewski, M.; Milczarek, M.; et al. Deformation Mechanisms of (100) and (110) Single-Crystal BCC Gum Metal Studied by Nanoindentation and Micropillar Compression. *Metall. Mater. Trans. A* **2024**, *55*, 4954–4964.
64. Sankaran, R.P.; Ozdol, V.B.; Ophus, C.; et al. Multiscale analysis of nanoindentation-induced defect structures in gum metal. *Acta Mater.* **2018**, *151*, 334–346.
65. Yang, Y.; Xu, D.; Cao, S.; et al. Effect of strain rate and temperature on the deformation behavior in a Ti-23.1Nb-2.0Zr-1.0O titanium alloy. *J. Mater. Sci. Technol.* **2021**, *73*, 52–60.
66. Yang, Y.; Zhang, B.; Meng, Z.; et al. {332}<113> Twinning transfer behavior and its effect on the twin shape in a beta-type Ti-23.1Nb-2.0Zr-1.0O alloy. *J. Mater. Sci. Technol.* **2021**, *91*, 58–66.
67. da Silva, M.R.; Plaine, A.H.; Pinotti, V.E.; et al. A review of Gum Metal: Developments over the years and new perspectives. *J. Mater. Res.* **2023**, *38*, 96–111.
68. Kanapaakala, G.; Subramani, V. A comprehensive review of Gum metal's potential as a biomedical material. Proceedings of the Institution of Mechanical Engineers. *Part L J. Mater. Des. Appl.* **2024**, *238*, 1200–1225.
69. Yuan, S.; Lin, N.; Zeng, Q.; et al. Recent advances in gum metal: Synthesis, performance and application. *Crit. Rev. Solid State Mater. Sci.* **2023**, *48*, 257–288.
70. Tong, Y.X.; Gu, H.L.; James, R.D.; et al. Novel TiNiCuNb shape memory alloys with excellent thermal cycling stability. *J. Alloys Compd.* **2019**, *782*, 343–347.
71. Gomez-Cort, J.F.; Czaja, P.; Szczerba, M.J.; et al. Extremely stable stress-induced martensitic transformation at the nanoscale during superelastic cycling of $Ni_{51}Mn_{28}Ga_{21}$ shape memory alloy. *Mater. Sci. Eng. A* **2023**, *881*, 145339.
72. Jaronie, M.J.; Martin, L.; Aleksandar, S.; et al. A review of shape memory alloy research, applications and opportunities. *Mater. Des.* **2013**, *56*, 1078–1113.
73. Guo, J.P.; Wei, Z.Y.; Shen, Y.; et al. Low-temperature superelasticity and elastocaloric effect in textured Ni–Mn–Ga–Cu shape memory alloys. *Scr. Mater.* **2020**, *185*, 56–60.
74. Dunand, D.C.; Müllner, P. Size effects on magnetic actuation in Ni-Mn-Ga shape-memory alloys. *Adv. Mater.* **2011**, *23*, 216–232.
75. Tian, Y.; Hu, B.; Dang, P.; et al. Noise-Aware Active Learning to Develop High-Temperature Shape Memory Alloys with Large Latent Heat. *Adv. Sci.* **2024**, *11*, 2406216.
76. Checa, P.; Feuchtwanger, J.; Musiienko, D.; et al. High temperature $Ni_{45}Co_5Mn_{25-x}Fe_xGa_{20}Cu_5$ ferromagnetic shape memory alloys. *Scr. Mater.* **2017**, *134*, 119–122.
77. Müllner, P. Magnetic Interactions of Disconnections and Fatigue of Ni-Mn-Ga. *Acta Mater.* **2025**, *298*, 121414.
78. Li, X.; Wang, K.; Li, Y.; et al. Mechanical and Magnetic Properties of Porous $Ni_{50}Mn_{28}Ga_{22}$ Shape Memory Alloy. *Metals* **2024**, *14*, 291.
79. Ding, Z.Y.; Liu, D.X.; Qi, Q.L.; et al. Multistep superelasticity of Ni-Mn-Ga and Ni-Mn-Ga-Co-Cu microwires under stress-temperature coupling. *Acta Mater.* **2017**, *140*, 326–336.
80. Zhang, X.X.; Witherspoon, C.; Müllner, P.; et al. Effect of pore architecture on magnetic-field-induced strain in polycrystalline Ni–Mn–Ga. *Acta Mater.* **2010**, *59*, 2229–2239.
81. Wang, K.Y.; Hou, R.H.; Xuan, J.M.; et al. Shape memory effect and superelasticity of $Ni_{50}Mn_{30}Ga_{20}$ porous alloy prepared by imitation casting method. *Intermetallics* **2022**, *149*, 1007668.
82. Salaheldeen, M.; Zhukova, V.; Blanco, J.M.; et al. The impact of high-temperature annealing on magnetic properties, structure and martensitic transformation of Ni_2MnGa-based glass-coated microwires. *Ceram. Int.* **2025**, *51*, 4378–4387.

83. Zhang, J.X.; Ding, Z.Y.; Hou, R.H.; et al. Giant high temperature superelasticity in $Ni_{53}Mn_{24}Ga_{21}Co_1Cu_1$ microwires. *Intermetallics* **2020**, *122*, 106799.
84. Ueland, S.M.; Schuh, A.C. Superelasticity and fatigue in oligocrystalline shape memory alloy microwires. *Acta Mater.* **2012**, *60*, 282–292.
85. Chen, Z.; Cong, D.; Ren, Y.; et al. Ferroelastic oligocrystalline microwire with unprecedented high-temperature superelastic and shape memory effects. *NPG Asia Mater.* **2022**, *14*, 17.
86. Lee, W.J.; Weber, B.; Leinenbach, C.; et al. Recovery stress formation in a restrained Fe–Mn–Si-based shape memory alloy used for prestressing or mechanical joining. *Constr. Build. Mater.* **2015**, *95*, 600–610.
87. Cassinerio, J.; Giordana, M.F.; Zelaya, E.; et al. On the impact of γ precipitates on the transformation temperatures in Fe–Ni–Co–Al–Ti–B shape memory alloy wires. *Shape Mem. Superelasticity* **2024**, *10*, 37–44.
88. Lehnert, R.; Müller, M.; Vollmer, M.; et al. On the influence of crystallographic orientation on superelasticity—Fe-Mn-Al-Ni shape memory alloys studied by advanced in situ characterization techniques. *Mater. Sci. Eng. A* **2023**, *871*, 144830.
89. Vollmer, M.; Arold, T.; Kriegel, M.J.; et al. Promoting abnormal grain growth in Fe-based shape memory alloys through compositional adjustments. *Nat. Commun.* **2019**, *10*, 2337.
90. Felice, I.O.; Shen, J.J.; Barragan, A.; et al. Wire and arc additive manufacturing of Fe-based shape memory alloys: Microstructure, mechanical and functional behavior. *Mater. Des.* **2023**, *231*, 112004.
91. Zhao, G.D.; Cui, Y.; Zhang, Y.; et al. Abnormal grain growth of FeMnAlNiCo shape memory alloys during directional recrystallisation. *J. Mater. Res. Technol.* **2023**, *23*, 819–829.
92. Yuan, W.; Shi, F.; Zhang, C.; et al. Influence of cyclic degradation behaviors in shape memory alloy on the seismic performance of structures. *J. Build. Eng.* **2025**, *111*, 113461.
93. Hamidreza, K.; Mahmoud, N.; Faezeh, K.J.; et al. The effect of high-pressure torsion on the microstructure and outstanding pseudoelasticity of a ternary Fe–Ni–Mn shape memory alloy. *Mater. Sci. Eng. A* **2021**, *802*, 140647.
94. Ding, Z.; Lv, X.; Wang, D.; et al. Multi-step phase-transformation of Ni-Mn-Ga smart microwires under stress-and strain-controlled tensile modes. *Smart Mater. Struct.* **2025**, *34*, 065032.
95. Hilscher, M.; Jübner, P.; Ghafoori, E. Iron-Based Shape Memory Alloys in Construction: A Review of Research, Applications, and Challenges. *Shape Mem. Superelasticity* **2025**, 1–15. https://doi.org/10.1007/s40830-025-00560-x.
96. Golrang, M.; Mohri, M.; Ghafoori, E.; et al. Tailoring functional properties of a FeMnSi shape memory alloy through thermo-mechanical processing. *J. Mater. Res. Technol.* **2024**, *291*, 1887–1900.
97. Abuzaid, W.; Sehitoglu, H.Y. Superelasticity and functional fatigue of single crystalline FeNiCoAlTi iron-based shape memory alloy. *Mater. Des.* **2018**, *160*, 642–651.
98. Deng, L.; Luo, J.; Li, R.; et al. Microstructural Evolution and Twinning Mechanism in Cold-Drawn CoNiV Medium-Entropy Alloy. *Smart Mater. Devices* **2025**, *1*, 2.
99. Sozinov, A.; Lanska, N.; Soroka, A.; et al. 12% magnetic field-induced strain in Ni-Mn-Ga-based non-modulated martensite. *Appl. Phys. Lett.* **2013**, *102*, 021902.
100. Vronka, M.; Straka, L.; Klementová; M; et al. Unexpected modulation revealed by electron diffraction in Ni-Mn-Ga-Co-Cu tetragonal martensite exhibiting giant magnetic field-induced strain. *Scr. Mater.* **2024**, *242*, 115901.
101. Petr, C.; Daria, D.; Kristian, M.; et al. Exceptionally small Young modulus in 10M martensite of Ni-Mn-Ga exhibiting magnetic shape memory effect. *Acta Mater.* **2023**, *257*, 119–133.
102. Yu, Q.; Wang, J.; Liang, C.; et al. A Giant Magneto-Superelasticity of 5% Enabled by Introducing Ordered Dislocations in $Ni_{34}Co_8Cu_8Mn_{36}Ga_{14}$ Single Crystal. *Adv. Sci.* **2024**, *240*, 1–9.
103. Zhen, L.Z.; Zong, L.B.; Yun, L.Z.; et al. Enhanced elastocaloric effect and refrigeration properties in a Si-doped Ni-Mn-In shape memory alloy. *J. Mater. Sci. Technol.* **2022**, *117*, 167–173.
104. Alexei, S.; Likhachev, A.A.; Ullakko, K.; et al. Magnetic and magnetomechanical properties of Ni-Mn-Ga alloys with easy axis and easy plane of magnetization. *Smart Mater. Struct.* **2001**, *4333*, 189–196.
105. Qu, Y.; Cong, D.; Li, S.; et al. Simultaneously achieved large reversible elastocaloric and magnetocaloric effects and their coupling in a magnetic shape memory alloy. *Acta Mater.* **2018**, *151*, 41–55.
106. Peng, C.T.; Zhen, Z.J.; Jia, X.; et al. Combining magnetocaloric and elastocaloric effects in a $Ni_{45}Co_5Mn_{37}In_{13}$ alloy. *J. Mater. Sci. Technol.* **2021**, *94*, 47–52.
107. Shi, Z.J.; Ming, Q.F.; Jie, Z.R.; et al. Microstructure and magnetocaloric effect in nonequilibrium solidified Ni-Mn-Sn-Co alloy prepared by laser powder bed fusion. *Addit. Manuf.* **2024**, *79*, 103941.
108. Wen, S.; Xiang, W.L.; Zhi, Y.; et al. Multicaloric effect in Ni-Mn-Sn metamagnetic shape memory alloys by laser powder bed fusion. *Addit. Manuf.* **2022**, *59*, 103125.
109. Leinenbach, C.; Kramer, H.; Bernhard, C.; et al. Thermo-Mechanical Properties of an Fe-Mn-Si-Cr-Ni-VC Shape Memory Alloy with Low Transformation Temperature. *Adv. Eng. Mater.* **2012**, *14*, 62–67.
110. Lee, J.W.; Weber, B.; Feltrin, G.; et al. Stress recovery behaviour of an Fe-Mn-Si-Cr-Ni-VC shape memory alloy used for prestressing. *Smart Mater. Struct.* **2013**, *22*, 125037.